

AD-A208 943

APPROVED FOR PUBLIC RELEASE;  
DISTRIBUTION UNLIMITED


89 6 13 078

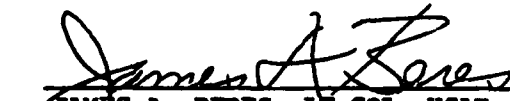
This report was submitted by The Aerospace Corporation, El Segundo, CA 90245, under Contract No. F04701-85-C-0086-P00019 with the Space Division, P.O. Box 92960, Los Angeles, CA 90009. It was reviewed and approved for The Aerospace Corporation by H. R. Rugge, Director, Space Sciences Laboratory.

Lt. Tyron Fisher was the project officer for the Mission-Oriented Investigation and Experimentation (MOIE) Program.

This report has been reviewed by the Public Affairs Office (PAS) and is releasable to the National Technical Information Service (NTIS). At NTIS, it will be available to the general public, including foreign nationals.

This technical report has been reviewed and is approved for publication. Publication of this report does not constitute Air Force approval of the report's findings or conclusions. It is published only for the exchange and stimulation of ideas.

  
\_\_\_\_\_  
TYRON FISHER, Lt, USAF  
MOIE Project Officer  
SSD/CLFPO

  
\_\_\_\_\_  
JAMES A. BERES, LT COL, USAF  
MOIE Program Manager  
AFSTC/WCO OL-AB

UNCLASSIFIED

SECURITY CLASSIFICATION OF THIS PAGE

## REPORT DOCUMENTATION PAGE

1a. REPORT SECURITY CLASSIFICATION <b>Unclassified</b>			1b. RESTRICTIVE MARKINGS	
2a. SECURITY CLASSIFICATION AUTHORITY			3. DISTRIBUTION/AVAILABILITY OF REPORT Approved for public release; distribution is unlimited.	
2b. DECLASSIFICATION/DOWNGRADING SCHEDULE				
4. PERFORMING ORGANIZATION REPORT NUMBER(S) <b>TR-0088(3940-06)-7</b>			5. MONITORING ORGANIZATION REPORT NUMBER(S) <b>SD-TR-89-35</b>	
6a. NAME OF PERFORMING ORGANIZATION <b>The Aerospace Corporation Laboratory Operations</b>		6b. OFFICE SYMBOL (If applicable)	7a. NAME OF MONITORING ORGANIZATION <b>Space Systems Division</b>	
6c. ADDRESS (City, State, and ZIP Code) <b>El Segundo, CA 90245</b>			7b. ADDRESS (City, State, and ZIP Code) <b>Los Angeles Air Force Base Los Angeles, CA 90009-2960</b>	
8a. NAME OF FUNDING/SPONSORING ORGANIZATION		8b. OFFICE SYMBOL (If applicable)	9. PROCUREMENT INSTRUMENT IDENTIFICATION NUMBER <b>F04701-85-C-0086-P00019</b>	
8c. ADDRESS (City, State, and ZIP Code)			10. SOURCE OF FUNDING NUMBERS	
			PROGRAM ELEMENT NO.	PROJECT NO.
			TASK NO.	WORK UNIT ACCESSION NO.
11. TITLE (Include Security Classification) <b>PRODUCTION OF VERY ENERGETIC ELECTRONS IN A DISCRETE AURORA</b>				
12. PERSONAL AUTHOR(S) <b>Swift, D. W., and Gorney, D. J.</b>				
13a. TYPE OF REPORT		13b. TIME COVERED FROM _____ TO _____		14. DATE OF REPORT (Year, Month, Day) <b>1989 April 26</b>
				15. PAGE COUNT <b>20</b>
16. SUPPLEMENTARY NOTATION				
17. COSATI CODES				
FIELD	GROUP	SUB-GROUP	18. SUBJECT TERMS (Continue on reverse if necessary and identify by block number)	
			Aurora ; Electron acceleration ; Plasma waves ; Magnetosphere ; Wave-particle interactions ; Electron beams . (phd) ←	
19. ABSTRACT (Continue on reverse if necessary and identify by block number)				
<p>Data are presented showing that acceleration of electrons to energies in excess of 100 keV sometimes occurs on field lines associated with discrete auroral arcs. Velocity distributions suggest that acceleration is in directions primarily perpendicular to the magnetic field. The examples studied in the S3-3 data set indicate that the process can occur in the altitude range from the topside ionosphere to 5500 km. Our favored explanation is that the field-aligned beam excites upper hybrid waves when it interacts with the dense ionospheric plasma. The waves efficiently scatter the beam both in energy and pitch angle.</p> <p>Keywords: /</p>				
20. DISTRIBUTION/AVAILABILITY OF ABSTRACT <input checked="" type="checkbox"/> UNCLASSIFIED/UNLIMITED <input type="checkbox"/> SAME AS RPT. <input type="checkbox"/> DTIC USERS			21. ABSTRACT SECURITY CLASSIFICATION <b>Unclassified</b>	
22a. NAME OF RESPONSIBLE INDIVIDUAL			22b. TELEPHONE (Include Area Code)	22c. OFFICE SYMBOL

## PREFACE

The portion of the research carried out by D.W. S. was supported by the Air Force Office of Scientific Research under Grant AFOSR 86-0037 and by the National Science Foundation under Grant ATM-86-18754. Work at The Aerospace Corporation was supported by the Space Division of the U.S. Air Force Systems Command under contract F04701-85-C-0086-P00019.

Accession For	
NTIS	<input checked="" type="checkbox"/>
DTIC	<input type="checkbox"/>
Unpublished	<input type="checkbox"/>
Justification	
By	
Date	
Approved	
Dist	
A-1	



## CONTENTS

1. INTRODUCTION .....	5
2. S3-3 OBSERVATIONS .....	7
3. DISCUSSION AND CONCLUSIONS .....	17
REFERENCES .....	19

## FIGURES

1. An $E - t$ Spectrogram of the Day 211 1976 Event, Which is Seen in the Electron Channel at 41270 UT .....	8
2. Plots of the Count Rates on the 12, 33, and 235 keV Channels .....	9
3. Electron Velocity Distribution Function Taken During the Event shown in Figs. 1 & 2 .....	10
4. Plot of the Electric Potential Associated with the Event Shown in the Three Previous Figures .....	11
5. An $E - t$ Spectrogram of the Day 98 1977 Events, Which are Seen in the Electron Channel at 59010, 59370, and Possibly 59415 UT. ....	12
6. Plots of the Count Rates on the 33 and 235 keV Channels .....	13
7. Same as Fig. 3, Except for the Electron Velocity Distribution Function Taken During the 59370 UT shown in Figs. 5 and 6 .....	14
8. Plot of the Electric Potential Associated with the 59370 UT Event Shown in the Three Previous Figures .....	15

## 1. INTRODUCTION

There are basically two types of aurora. One is the diffuse aurora, which is caused by the precipitation of trapped electrons, and the other is the discrete aurora, which is caused by electrons accelerated through a field-aligned potential drop. The two types of precipitation are easily distinguished in satellite observations from the characteristics of the energy spectra. The diffuse aurora has a nearly isotropic pitch angle distribution and has an energy spectrum extending monotonically to many tens of keV, and the fluxes are seen to change relatively slowly over traverses of several degrees in latitude. The discrete aurora lies poleward of the diffuse aurora and is characterized by large spatial variability and by spectral distributions peaked in energy. These structures seen on an  $E - t$  (Energy - time) spectrogram are referred to as inverted-V events [Frank and Akerson<sup>1</sup>]. At times a magnetic-field-aligned beam is seen, indicating that the electrons are accelerated through a field-aligned potential drop. The inverted-V events correlate very well with the occurrence of paired electrostatic shocks, first deduced by Wescott et al.<sup>2</sup> and later seen directly by Mozer et al.<sup>3</sup> on the S3-3 satellite.

Both ground-based observations of luminosity versus altitude and direct spectral measurements from rockets and satellites indicate that the energies of electrons responsible for the discrete aurora usually are in the range of a few keV, but rarely more than 10 keV. This is consistent with the voltage differences seen across the paired shocks [Mozer et al.<sup>4</sup>]. The purpose of this report is to document S3-3 satellite observations which show that at times a portion of the electrons in inverted-V events can be accelerated to energies considerably in excess of the likely accelerating potential.

The search for these events was motivated by numerical simulations of auroral electron precipitation by Swift.<sup>5</sup> These simulations indicated that under certain circumstances upper hybrid waves would be excited by a field-aligned auroral beam. The upper hybrid wave was found to be effective in scattering the electron beam in both energy and pitch angle. This scattering resulted in some electrons being diffused to energies considerably in excess of the beam energy. This is in contrast to atmospheric scattering, which can only degrade auroral electron energy. Therefore, these events should be easily seen in inverted-V events as electron fluxes with energies considerably in excess of the characteristic energy of the event.

The observations to be reported below are not the first observations of approximately 100 keV electrons in the discrete aurora. Evans<sup>6</sup> flew a rocket, instrumented with a series of channel multiplier detectors for  $E \leq 30$  keV and plastic scintillations for  $E > 60$  keV, into a bright discrete aurora with a background luminosity flickering at 10 Hz. A 6 keV monoenergetic component was detected. In addition, the flickering component was seen in the various energy channels with a modulation increasing with increasing energy up to 120 keV. It was determined from the lack of a velocity dispersion that the source region for the energetic component must have been within 1000 km of the detectors. The observations of

Evans prompted Perkins<sup>7</sup> to consider the interaction of an auroral electron beam with a dense ionospheric plasma. He found that upper hybrid waves would be excited, which would efficiently scatter the beam in both energy and pitch angle. Moreover, he was able to account for the 10 Hz periodicity in the energetic component.

Although the production of energetic electrons in the discrete aurora is not a new discovery, it is a phenomenon that has been ignored for the past twenty years. The reason, we suspect, is that with the introduction of the electrostatic analyzers capable of measuring particle fluxes in the keV energy range and below, investigators tended to ignore the older technology, which was capable of observing particle fluxes at energies of tens of keV and above. The production of the tens of keV and above electrons should make the discrete aurora easily visible in the X-ray wavelengths due to bremsstrahlung. Recent developments in the ability to image in the X-ray spectrum [Imhof et al.<sup>8</sup>, Rosenberg et al.<sup>9</sup>] should be cause for renewed interest in the production of highly energetic electrons in the discrete aurora. Also, of course, the physical processes which lead to acceleration of electrons to energies higher than the beam energy are of scientific interest in their own right.

## 2. S3-3 OBSERVATIONS

The presentation will consist of a fairly detailed exposition of two of our best documented examples from the S3-3 data set, followed by a more general discussion of other examples. Figure 1 shows an S3-3  $E - t$  spectrogram from Day 211 (July 29) in 1976. The spectrogram shows grey scale plots of electron (0.17 - 33.0 keV) and ion (0.09 - 3.9 keV) energy flux, and separate panels for the 235 keV electron channel and  $> 80$  keV proton channel. Filter outputs from the AC electric field (30 Hz - 100 kHz) are shown in the top panel. Ephemeris parameters are indicated at 200 sec intervals. The event occurs near 41270 UT, at an invariant latitude of  $75^\circ$  and a magnetic local time of 18.6 hr. It can be seen from the 235 keV channel that the satellite is well poleward of the plasma sheet and is passing through a broad inverted-V region with a characteristic energy of 4 to 8 keV. In the event at 41270, electron fluxes at all energies are enhanced, but the peak energy flux appears in the 33 keV channel, and there is even some enhanced flux in the 235 keV channel. It can also be seen that there is a coincident noise burst in the AC electrostatic field. This is likely noise generated by the auroral electron beam on the lower hybrid resonance curve; it cannot be on the upper hybrid curve, since the local upper hybrid frequency lies above the pass band of the AC electric field instrument.

Figure 2 shows count rates in the 12, 33, and 235 keV channels. Each point represents a quarter spin period of approximately 5 sec of data. Because of the greatly compressed time scale, the event is marked with an arrow. It shows up quite strongly in the 33 keV channel and is barely perceptible in the 235 keV channel. There is a more prominent peak in fluxes on the 235 keV channel at 41400, which has no corresponding signature on the  $E - t$  spectrogram.

Figure 3 is a contour plot showing the electron velocity distribution function. The most significant features are the contours going off-scale with asymptotes at  $20^\circ$  to the field line. Electrons with a pitch angle of  $20^\circ$  would mirror in a magnetic field intensity of  $B = 0.48$  G. This would place the source region for the particles at ionospheric altitudes. This feature began to appear in the third quadrant in the upgoing fluxes on the previous frame and was seen to be fully developed in the downgoing fluxes in the fourth quadrant. The event therefore began somewhere around 41251 UT. From Fig. 3, it can be seen that the event ended somewhere around 41280 UT, making an approximate 30 sec duration. The satellite in this time has a latitudinal displacement of about  $0.27^\circ$ , or 66 km. Since both upward and downward fluxes are seen, the event must be on closed field lines. The data does not directly indicate the hemisphere of origin. Assuming the magnetic field line crosses the plasma sheet at 10 RE, the field line path between conjugate ionospheres must be approximately 30 RE, so the bounce time between hemispheres of an electron moving at 105 km/sec is about 4 sec. This is less than a quarter scan on S3-3.



# S3-3 SATELLITE DAY 98, 1977

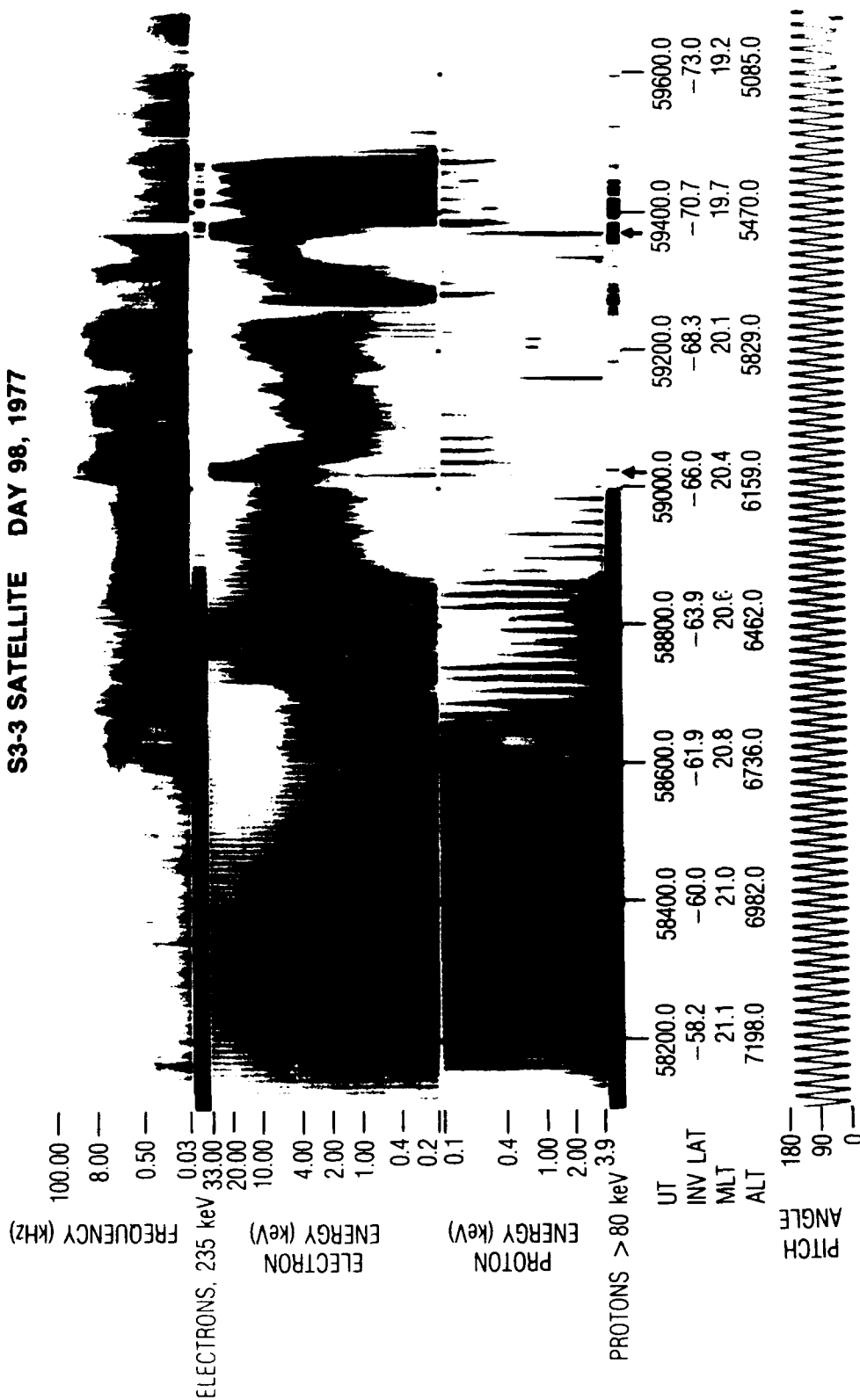


Fig. 1. An  $E-t$  Spectrogram of the Day 211 1976 Event, Which is Seen in the Electron Channel at 41270 UT.

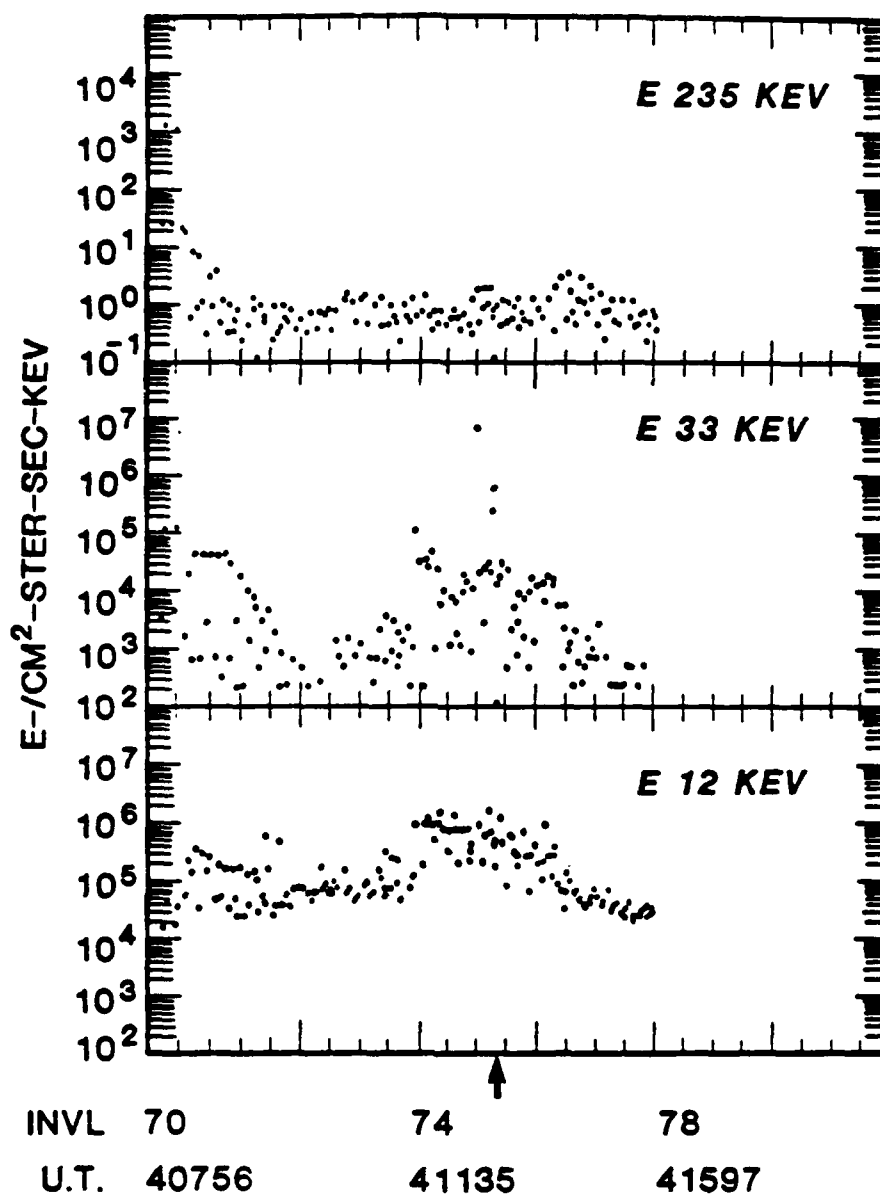


Fig 2. Plots of the Count Rates on the 12, 33, and 235 keV Channels. The time of the event is marked by the arrow. The event is particularly evident on the 33 keV channel. The peak fluxes at 33 keV are field aligned, both up and down, while at 235 keV the fluxes tend to be downward or perpendicular.

**ELECTRONS**  
**DAY 211 YEAR 1976**  
**41263 to 41285 U.T.**

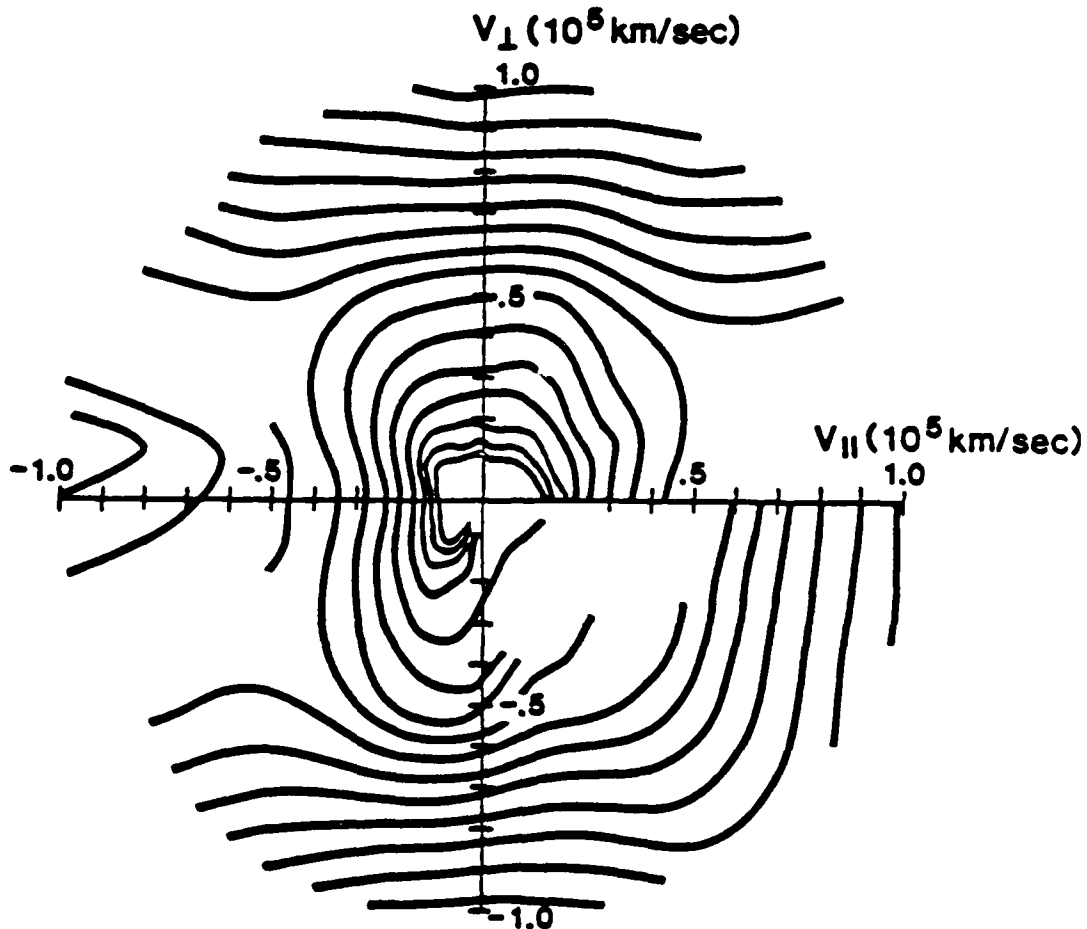


Fig 3. Electron Velocity Distribution Function Taken During the Event Shown in Figs. 1 and 2. The contour intervals are on a logarithmic scale. The distribution function is taken as the satellite scans in pitch angle going counter-clockwise from the  $V_{\perp}$  axis. Positive  $V_{\perp}$  is parallel to the magnetic field and downward in the northern hemisphere. A pitch angle sweep takes 22 sec.

Figure 4 shows the electrostatic potential measured along the satellite trajectory through this event. There is an obvious 8 kV dip in the curve, which begins at approximately 41244 and ends at 41255 UT, an approximate 10 sec duration. Since the satellite is traveling poleward, the position of the potential dip is largely equatorward of the highly energetic portion of the precipitation event.

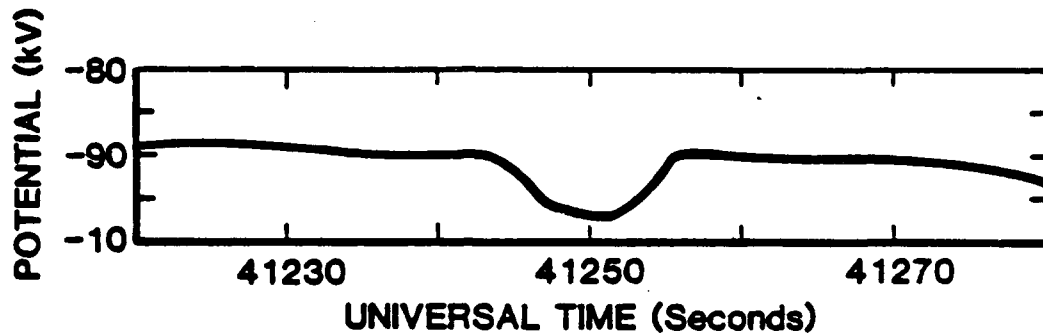


Fig. 4. Plot of the Electric Potential Associated with the Event Shown in the Three Previous Figures.

The  $E - t$  spectrogram of Fig. 5 shows two events at 59010 and 59370 UT of day 98 (April 8) 1978. There is possibly a third and very narrow event at 59415 UT. This pass was in the southern hemisphere, and the two major events observed were at 6159 and 5500 km altitudes at latitudes of  $66^\circ$  and  $70.1^\circ$ , respectively. The 59370 event also shows up clearly on the 235 keV channel. The AC electric field detector was unable to operate during this extremely energetic event. Figure 6 shows the count rates on the 33 keV and 235 keV channels. (The 12 keV channel had failed.) The 33 keV channel shows large responses to the three events. The 235 keV channel shows no response in the first event, but has a broad response spanning the time of the latter two events. There is a single data point that stands out above the envelope of the other points at the time of the second event.

Figure 7 shows the velocity distribution of the second event, taken between 59368 and 59385 UT. The most prominent feature is the large anisotropy favoring perpendicular energies. This suggests that the satellite is in the source region of the energetic electrons. The frame for the previous satellite spin showed rather low count rates, and the following frame showed upward-directed fluxes at an angle of  $55^\circ$  to the magnetic field, indicating the source region had moved into a region where the field intensity was 0.13 G, corresponding to an altitude of about 4000 km.

Figure 8 shows the potential deduced from the electric field measurement along the satellite track. The event occurred just after the satellite had passed through a 13 kV jump in potential. It is curious that the energetic electron event in this and the previous example occurred just poleward, rather than in the middle of the potential dip.

# S3-3 SATELLITE DAY 211, 1976

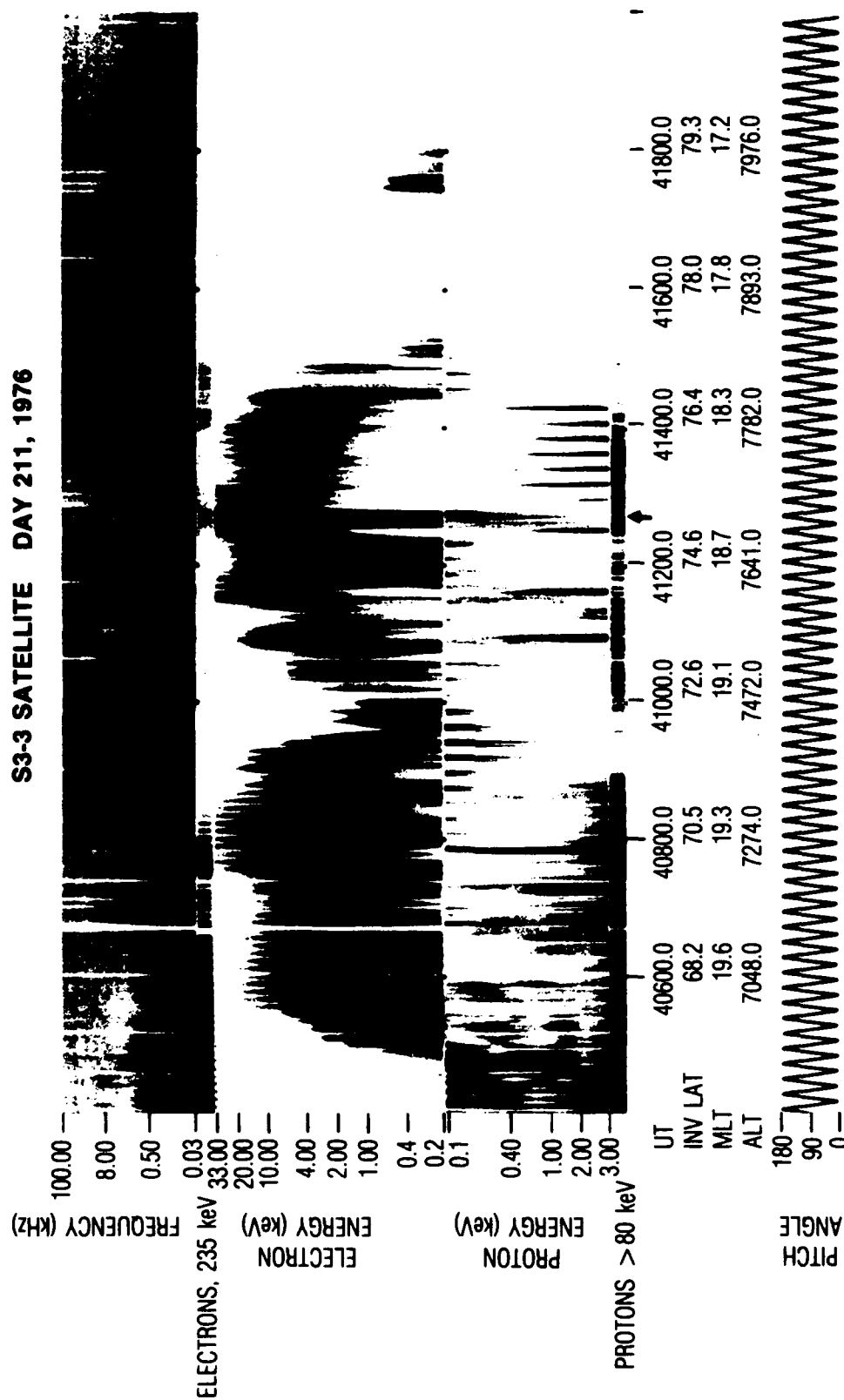


Fig. 5. An  $E-t$  Spectrogram of the Day 98 1977 Events, Which are Seen in the Electron at 59010, 59370, and Possibly 59415 UT.

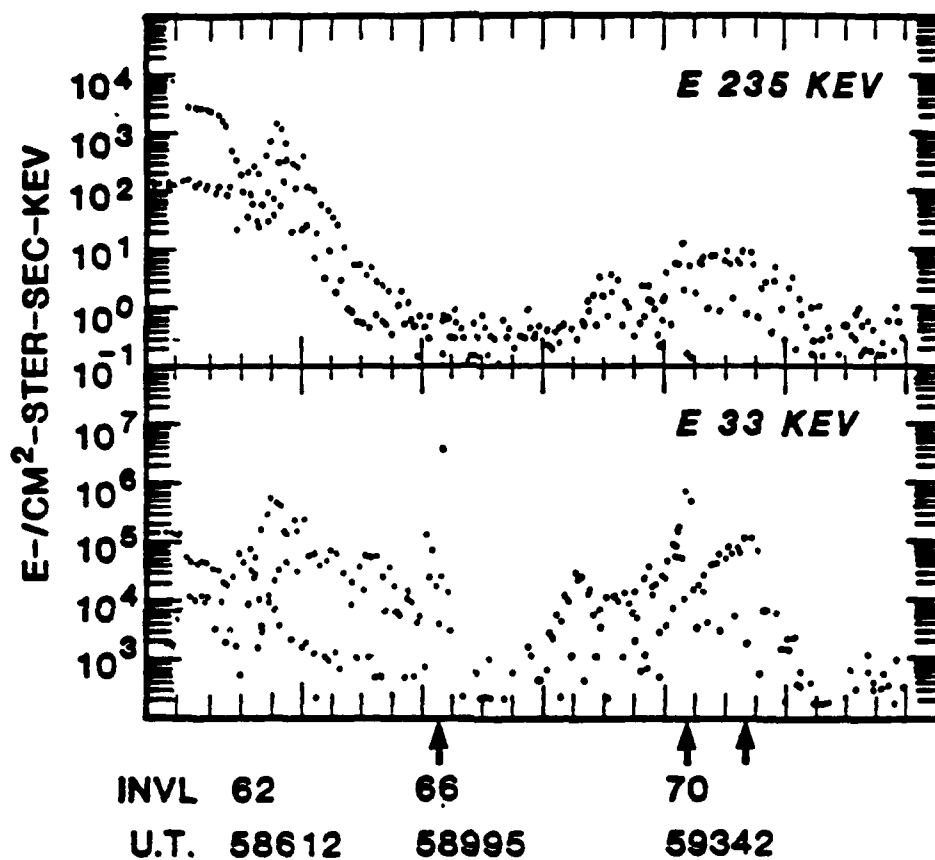


Fig. 6. Plots of the Count Rates on the 33 and 235 keV channels. The events are evident on the 33 keV channel and there is a one-point peak corresponding to the 59370 UT event on the 235 keV channel. This is embedded in a broader region of enhanced fluxes on the 235 keV channel.

**ELECTRONS**  
**DAY 98 YEAR 1977**  
**59368 to 59385 U.T.**

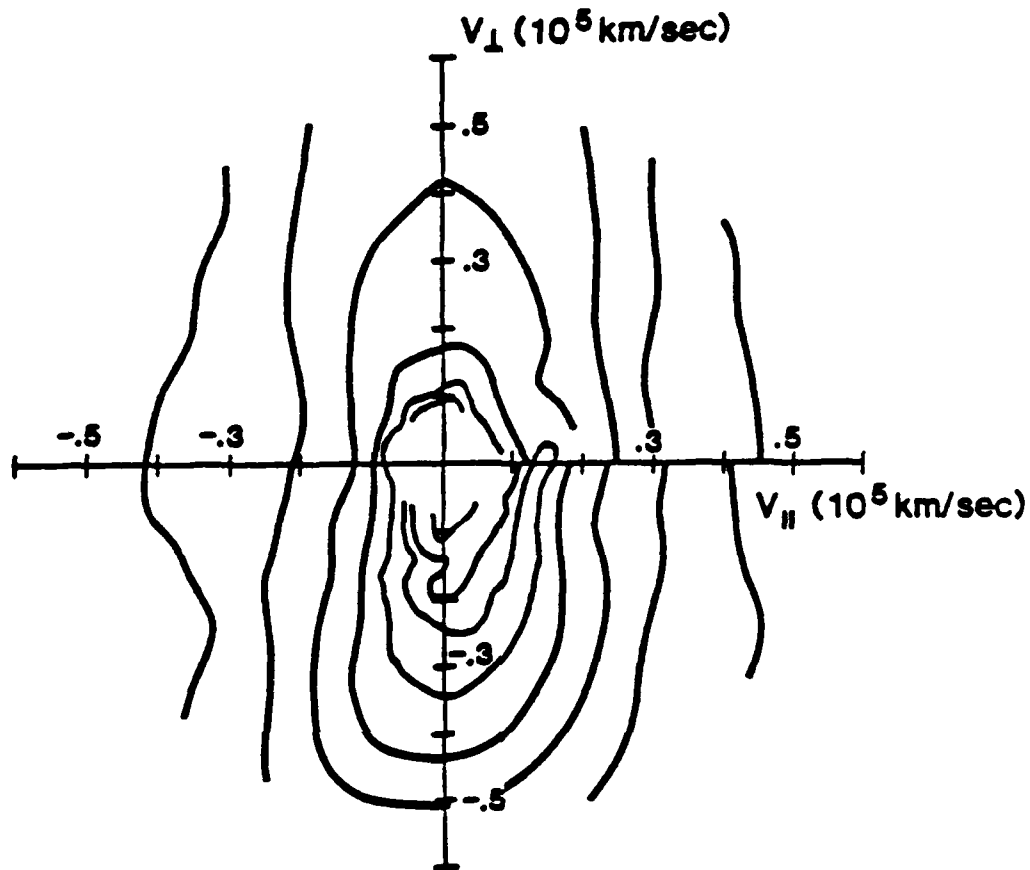


Fig. 7 Same as Fig. 3, Except for the Electron Velocity Distribution Function Taken During the 59370 UT Event Shown in Figs. 5 and 6. A pitch angle sweep takes 17 sec.

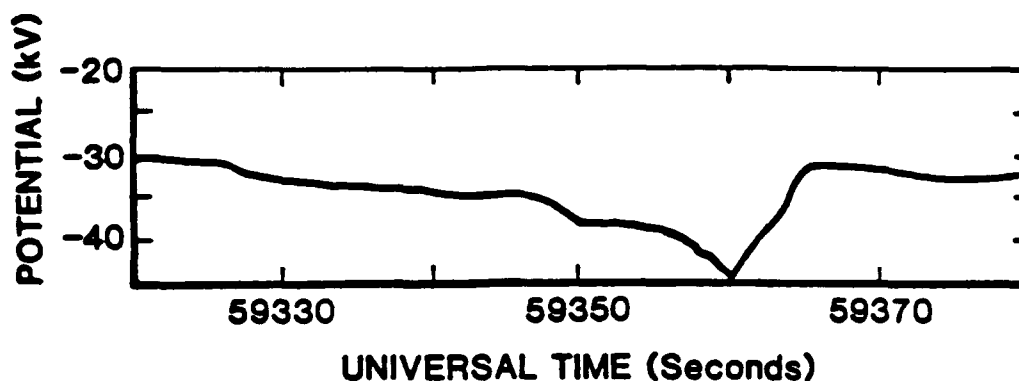


Fig. 8. Plot of the Electric Potential Associated with the 59370 UT Event Shown in the Three Previous Figures.

Table 1 presents a summary of the events that have been identified by responses in the 33 keV channel in the S3-3 data set at The Aerospace Corporation. The column labeled 235 keV indicates whether there was any enhancement in the fluxes in this channel associated with the event. A blank indicates the unavailability of data. The column headed by  $\Phi$  indicates the maximum potential change associated with the event, while the  $\alpha$ -column indicates the pitch angle of the electron conic. The particular signature for the events is evidence that electrons have been scattered to energies considerably in excess of the likely accelerating potential. Another criterion was that the events had to be in a region of inverted-V precipitation and well poleward of the trapped radiation. In order to be identified, the event had to have a duration on the spectrogram of a spin period or longer. This meant that it had to have a width of several tens of kilometers, much larger than the widths associated with discrete auroral arcs. Appearance of enhanced fluxes on the 235 keV channel served as confirming evidence. The selection procedure undoubtedly missed a considerable portion of the events, so the table should not be used to infer occurrence statistics. However, the occurrence frequency of the highly energetic events appears to be much lower than for the inverted-V events. The events that have been identified occurred during the evening and morning hours, and during a time when the ionospheric footprint was sunlit. We do not know whether this is significant because most of the S3-3 data set scanned for these events was under daylight conditions. The scanty pitch angle data indicate that the scattering process took place between altitudes of a few hundred km and 5500 km. Although the individual velocity distributions contain both upgoing and downgoing particles, indicating the presence of particles reflected from the conjugate hemisphere, we feel that the events occurred in the hemisphere in which they were observed. One reason is that enhancement of low-energy fluxes, down to 200 eV, is also observed. The transit time of these fluxes from one hemisphere to another is about 22 sec, which should produce a noticeable dispersion if the source were in the opposite hemisphere. We are also able to discern instances in which fluxes are seen in the 235 keV channel, but there is no simultaneous fea-



instances in which fluxes are seen in the 235 keV channel, but there is no simultaneous feature in the  $E - t$  spectrogram. We suspect these may be events which occur in the opposite hemisphere.

Table 1. A Catalog of Energetic Events Identified in the S3-3 Data Set.

Year	Day	UT	INVL	MLT	Alt.	235 keV	$\Phi$	$\alpha$
1976	210	52200	73.2	20.0	7450	?	2 kV	-
1976	211	41270	75.	18.6	7660	yes	8 kV	20°
1977	98	59010	-66.	20.4	6159	no	4 kV	40°
1977	98	59370	-70.1	20.2	5500	yes	13 kV	90°
1978	93	76320	69.	17.5	2350	yes	-	-
1978	93	77910	70.	6.4	6000	yes	-	-
1978	94	72660	63.5	17.7	2600	yes	-	-
1978	104	18880	74.	8.1	6550	?	-	-

### 3. DISCUSSION AND CONCLUSIONS

We have presented observations indicating that electrons with energies considerably in excess of the accelerating potential may be produced in the discrete aurora. The observations of the distribution function also indicate that much of the energy appears in the perpendicular motion. The potential that accelerates the electrons would create primarily a field-aligned beam. Such a beam interacting with the ionospheric electrons can excite Langmuir waves and waves on the lower and upper hybrid resonance cones. The analysis of Maggs [1978] and the simulations of Swift [1988] indicate that inhomogeneities perpendicular to the magnetic field will suppress the Langmuir wave. Waves on the lower hybrid cone, which can propagate away from the cone in the whistler mode, are believed to be responsible for auroral hiss. Both these and the Langmuir waves will heat the beam in directions primarily parallel to the magnetic field, so it is unlikely that these waves can be responsible for the strong perpendicular heating. The analysis of Perkins [1968] and the simulations of Swift show that waves on the upper hybrid branch do interact with electrons through gyroresonance to produce strong perpendicular heating.

Observational evidence for the presence of upper hybrid waves in regions of auroral precipitation is rather scanty. However, Kellogg et al. [1978] report the observation of intense emissions at 2.3 mHz at 328 km altitude which coincide with bursts of electron fluxes. The authors speculate the waves were generated at higher altitude on the upper hybrid resonance cone and propagated to the observing rocket in the Z-mode. More recently, satellite data of electron fluxes and plasma waves presented by Beghin et al. [1988] showed an example of precipitation of 20 keV electrons coinciding with an electrostatic wave burst above the local plasma frequency.

One likely reason why the energetic electron events are not seen more often is that the upper hybrid waves must compete with lower hybrid waves for the same energy source, namely the field-aligned electron beam. Maggs [1978] has shown that when the local gyrofrequency exceeds the plasma frequency, waves on the lower hybrid resonance cone are favored; whereas waves on the upper hybrid branch are favored when the plasma frequency exceeds the gyrofrequency. The simulation results of Swift [1988] also indicate this trend. This may explain why the events reported in this data set occurred during times when the ionosphere was likely to be sunlit. Moreover, because of the generally low plasma densities in the ionosphere, it is not common for the electron plasma frequency to exceed the gyrofrequency. This may explain the relative scarcity of the energetic electron events. However, it should be noted that the observations of Evans [1967] and Kellogg et al. [1978] were in a darkened ionosphere; they may have been in an aurorally enhanced ionosphere, and there may have been special geometrical conditions that would have favored the upper hybrid waves.

The S3-3 data set is not well adapted to obtain good statistics on the occurrence frequency of the energetic electron events. The ideal instrument for obtaining this information

the aurora bombarded with the energetic electrons discussed in this report should readily show up as discrete structures in X-ray images of the type displayed by Imhof et al. and comparison between the visible and X-ray images should provide a good indication of the occurrence frequency and spatial extent of the events. However, it might be desirable to look at X-ray energies higher than the 4 keV used by Imhof et al. in order to discriminate against X-rays that could have been produced by electrons with energies typical of inverted-V electrons.

## REFERENCES

1. L. A. Frank and K. L. Ackerson, "Observation of Charged Particle Precipitation in the Auroral Zones," *J. Geophys. Res.* **76**, 3612, (1971).
2. E. M. Wescott, et al., "The Skylab Barium Injection Experiments, 2, Evidence for a Double Layer," *J. Geophys. Res.* **81**, 4495, (1976).
3. F. S. Mozer, et al., "Evidence for Paired Electrostatic Shocks in the Polar Magnetosphere," *Phys. Rev. Lett.* **38**, 292, (1977).
4. F. S. Mozer, et al., "Satellite Measurements and Theories of Low Altitude Auroral Particle Acceleration," *Space Sci. Rev.* **27**, 155, (1980).
5. D. W. Swift, "A Numerical Model for Auroral Precipitation," *J. Geophys. Res.* **93** (in press), (1988).
6. D. S. Evans, "A 10-cps Periodicity in the Precipitation of Auroral Zone Electrons," *J. Geophys. Res.* **72**, 4281, (1967).
7. F. W. Perkins, "Plasma Wave Instabilities in the Ionosphere Over the Aurora," *J. Geophys. Res.* **73**, 6631, (1968).
8. Imhof, W. L., et al., "Bremsstrahlung X-ray Images of Isolated Electron Patches at High Latitudes," *J. Geophys. Res.* **90**, 6515, (1985).
9. Rosenberg, T. J., et al., "Coordinated Ground and Space Measurements of an Auroral Arc over the South Pole," *J. Geophys. Res.* **92**, 11123, (1987).
10. Maggs, J. E., "Electrostatic Noise Generated by the Auroral Electron Beam," *J. Geophys. Res.* **83**, 3173, (1978).
11. Kellogg, P. J., S. J. Monson and B. A. Whalen, "Rocket Observations of High Frequency Waves Over a Strong Aurora," *Geophys. Res. Lett.* **5**, 47, (1978).
12. Beghin, C., J. L. Rauch and J. M. Bosqued, "Electrostatic Plasma Waves and RF Auroral Hiss Generated at Low Altitude," submitted to *J. Geophys. Res.*, (1988).

## LABORATORY OPERATIONS

The Aerospace Corporation functions as an "architect-engineer" for national security projects, specializing in advanced military space systems. Providing research support, the corporation's Laboratory Operations conducts experimental and theoretical investigations that focus on the application of scientific and technical advances to such systems. Vital to the success of these investigations is the technical staff's wide-ranging expertise and its ability to stay current with new developments. This expertise is enhanced by a research program aimed at dealing with the many problems associated with rapidly evolving space systems. Contributing their capabilities to the research effort are these individual laboratories:

Aerophysics Laboratory: Launch vehicle and reentry fluid mechanics, heat transfer and flight dynamics; chemical and electric propulsion, propellant chemistry, chemical dynamics, environmental chemistry, trace detection; spacecraft structural mechanics, contamination, thermal and structural control; high temperature thermomechanics, gas kinetics and radiation; cw and pulsed chemical and excimer laser development including chemical kinetics, spectroscopy, optical resonators, beam control, atmospheric propagation, laser effects and countermeasures.

Chemistry and Physics Laboratory: Atmospheric chemical reactions, atmospheric optics, light scattering, state-specific chemical reactions and radiative signatures of missile plumes, sensor out-of-field-of-view rejection, applied laser spectroscopy, laser chemistry, laser optoelectronics, solar cell physics, battery electrochemistry, space vacuum and radiation effects on materials, lubrication and surface phenomena, thermionic emission, photo-sensitive materials and detectors, atomic frequency standards, and environmental chemistry.

Computer Science Laboratory: Program verification, program translation, performance-sensitive system design, distributed architectures for spaceborne computers, fault-tolerant computer systems, artificial intelligence, micro-electronics applications, communication protocols, and computer security.

Electronics Research Laboratory: Microelectronics, solid-state device physics, compound semiconductors, radiation hardening; electro-optics, quantum electronics, solid-state lasers, optical propagation and communications; microwave semiconductor devices, microwave/millimeter wave measurements, diagnostics and radiometry, microwave/millimeter wave thermionic devices; atomic time and frequency standards; antennas, rf systems, electromagnetic propagation phenomena, space communication systems.

Materials Sciences Laboratory: Development of new materials: metals, alloys, ceramics, polymers and their composites, and new forms of carbon; non-destructive evaluation, component failure analysis and reliability; fracture mechanics and stress corrosion; analysis and evaluation of materials at cryogenic and elevated temperatures as well as in space and enemy-induced environments.

Space Sciences Laboratory: Magnetospheric, auroral and cosmic ray physics, wave-particle interactions, magnetospheric plasma waves; atmospheric and ionospheric physics, density and composition of the upper atmosphere, remote sensing using atmospheric radiation; solar physics, infrared astronomy, infrared signature analysis; effects of solar activity, magnetic storms and nuclear explosions on the earth's atmosphere, ionosphere and magnetosphere; effects of electromagnetic and particulate radiations on space systems; space instrumentation.